

Self-Conditioned Probabilistic Learning of Video Rescaling

Yuan Tian¹ Guo Lu² Xiongkuo Min¹ Zhaohui Che¹ Guangtao Zhai^{1*} Guodong Guo³ Zhiyong Gao¹

¹Shanghai Jiao Tong University ²Beijing Institute of Technology ³Baidu

{ee.tianyuan, minxiongkuo, chezhaohui, zhaiguangtao, zhiyong.gao}@sjtu.edu.cn

guo.lu@bit.edu.cn, guogudong01@baidu.com

Abstract

Bicubic downscaling is a prevalent technique used to reduce the video storage burden or to accelerate the downstream processing speed. However, the inverse upscaling step is non-trivial, and the downsampled video may also deteriorate the performance of downstream tasks. In this paper, we propose a self-conditioned probabilistic framework for video rescaling to learn the paired downscaling and upscaling procedures simultaneously. During the training, we decrease the entropy of the information lost in the downscaling by maximizing its probability conditioned on the strong spatial-temporal prior information within the downsampled video. After optimization, the downsampled video by our framework preserves more meaningful information, which is beneficial for both the upscaling step and the downstream tasks, e.g., video action recognition task. We further extend the framework to a lossy video compression system, in which a gradient estimator for non-differential industrial lossy codecs is proposed for the end-to-end training of the whole system. Extensive experimental results demonstrate the superiority of our approach on video rescaling, video compression, and efficient action recognition tasks.

1. Introduction

High-resolution videos are widely used over various computer vision tasks [46][64][8][37][35][52][66]. However, considering the increased storage burden or the high computational cost, it is usually required to first downscale the high-resolution videos. Then we can either compress the output low-resolution videos for saving storage cost or feed them to the downstream tasks to reduce the computational cost. Despite that this paradigm is prevalent, it has the following two disadvantages. First, it is non-trivial to restore the original high-resolution videos from the (compressed) low-resolution videos, even we use the latest super-resolution methods [32, 65, 50, 59]. Second, it is also a challenge for the downstream tasks to achieve high performance based on these low-resolution videos. Therefore,

it raises a question that whether the downscaling operation can facilitate the reconstruction of the high-resolution videos and also preserve the most meaningful information for the downstream tasks.

Recently, this question has been partially studied as a single image rescaling problem [26, 29, 49, 62], which learns the image downscaling and upscaling operators jointly. However, how to adapt these methods from image to video domain and leverage the rich temporal information within videos are still open problems. More importantly, modeling the lost information during downscaling is non-trivial. Current methods either ignore the lost information [26, 29, 49] or assume it as an independent distribution in the latent space [62], while neglecting the *internal relationship* between the downsampled image and the lost information. Besides, all literature mentioned above have not explored how to apply the rescaling technique to the lossy image/video compression.

In this paper, we focus on building a video rescaling framework and propose a self-conditioned probabilistic learning approach to learn a pair of video downscaling and upscaling operators by exploiting the information dependency within the video itself. Specifically, we first design a learnable frequency analyzer to decompose the original high-resolution video into its downsampled version and the corresponding high-frequency component. Then, a Gaussian mixture distribution is leveraged to model the high-frequency component by *conditioning* on the downsampled video. For accurate estimation of the distribution parameters, we further introduce the local and global temporal aggregation modules to fuse the spatial information from adjacent downsampled video frames. Finally, the original video can be restored by a frequency synthesizer from the downsampled video and the high-frequency component sampled from the distribution. We integrate the components above as a novel self-conditioned video rescaling framework termed **SelfC** and optimize it by minimizing the negative log-likelihood for the distribution.

Furthermore, we apply our proposed SelfC in two practical applications, *i.e.* lossy video compression and video

*Corresponding author.

action recognition. In particular, to integrate our framework with the existing non-differential video codecs (*e.g.*, H.264 [61] and H.265 [48]), we propose an efficient and effective one-pass optimization strategy based on the *control variates* method and approximate the gradients of traditional codecs in the back-propagation procedure, which formulates an end-to-end optimization system.

Experimental results demonstrate that the proposed framework achieves state-of-the-art performance on the video rescaling task. More importantly, we further demonstrate the effectiveness of the framework in practical applications. For the lossy video compression task, compared with directly compressing the high-resolution videos, the video compression system based on our SelfC framework cuts the storage cost significantly (up to 30% reduction). For the video action recognition task, our framework reduces more than 60% computational complexity with negligible performance degradation.

In summary, our main contributions are:

- We propose a probabilistic learning framework dubbed **SelfC** for the video rescaling task, which models the lost information during downscaling as a dynamic distribution conditioned on the downsampled video.
- Our approach exploits rich temporal information in downsampled videos for an accurate estimation of the distribution parameters by introducing the specified local and global temporal aggregation modules.
- We propose a gradient estimation method for non-differential lossy codecs based on the control variates method and Monte Carlo sampling technique, extending the framework to a video compression system.

2. Related Work

Video Upscaling after Downscaling. Traditional video downscaling approaches subsample the input high-resolution (HR) videos by a handcrafted kernel, such as Bilinear and Bicubic. For restoration, video super-resolution (SR) methods are utilized. Since the SR task is inherently ill-posed, previous SR works [32, 65, 50, 59, 18, 25] mainly leverage a heavy neural network to hallucinate the lost details, only achieving unsatisfactory results. Taking the video downscaling method into consideration may help mitigate the ill-posedness of the video upscaling procedure.

There are already a few works on single image rescaling task in a similar spirit, which consider the downscaling and the upscaling of the image simultaneously. For example, Kim *et al.* [26] proposed a task-aware downscaling model based on an auto-encoder framework. Later, Li *et al.* [29] proposed to use a convolution neural network (CNN) to estimate the downsampled low-resolution images for a given super-resolution method. For stereo matching task, Yang *et al.* [67] proposed a superpixel-based down-sampling/up-sampling scheme to effectively preserve object

boundaries and fine details. More recently, Xiao *et al.* [62] proposed to leverage an invertible neural network (INN) to model the two reciprocal steps, which relies on a very deep INN to map the complex distribution of the lost information to an *independent* and *fixed* normal distribution.

However, these methods neither leverage the temporal information between adjacent frames, which is important for video related tasks, nor consider the fact that the components of different frequencies in natural images or videos are conditionally dependent [55, 47, 40, 56].

Video Compression. Several traditional video compression algorithms have been proposed and widely deployed, such as H.264 [61] and H.265 [48]. Most of them follow the predictive coding architecture and rely on the sophisticated hand-crafted transformations to analyze the redundancy within the videos. Recently, fully end-to-end video codecs [16][7][68][3][31][33][21][36] such as DVC [34] have been proposed by considering the rate-distortion trade-off of the whole compression system. They demonstrate promising performance and may be further improved by feeding more ubiquitous videos in the wild. However, they haven't been widely used by industrial and are lack of the hardware implementation. In contrast, our framework can be readily integrated with the best traditional video codecs and further saves the storage space of the compressed video significantly.

Video Action Recognition. Simonyan *et al.* [46] first proposed the two-stream framework. Feichtenhofer *et al.* [10] then improved it. Later, Wang *et al.* [58] proposed a new sparse frame sampling strategy. Recently, 3D networks [53][6][17][54][41][9][51] also show promising performance. Our work can accelerate the off-the-shelf action CNNs by 3-4 times while reserving the comparable performance. We mainly conduct experiments on light-weight 2D action CNNs (*e.g.*, TSM [30]) based on 2D-ResNet50 [19] for efficiency.

3. Proposed Method

An overview of our proposed SelfC framework is shown in Fig. 1 (a). During the downscaling procedure, given a high-resolution (HR) video, a frequency analyzer (FA) (Section 3.1) first converts it into video features f , where the first 3 channels are low-frequency (LF) component f_l , the last $3 \cdot k^2$ channels are high-frequency (HF) component f_h , and k is the downscaling ratio. Then, f_l is quantized to a LR video x_l for storage. f_h is discarded in this procedure.

During the upscaling procedure, given the LR video x_l , the spatial-temporal prior network (STP-Net) (Section 3.3) predicts the probability density function of the HF component f_h :

$$p(f_h|x_l) = \text{STP-Net}(x_l). \quad (1)$$

We model $p(f_h|x_l)$ as a continuous mixture of the parametric Gaussian distributions (Section 3.2). Then, a case of

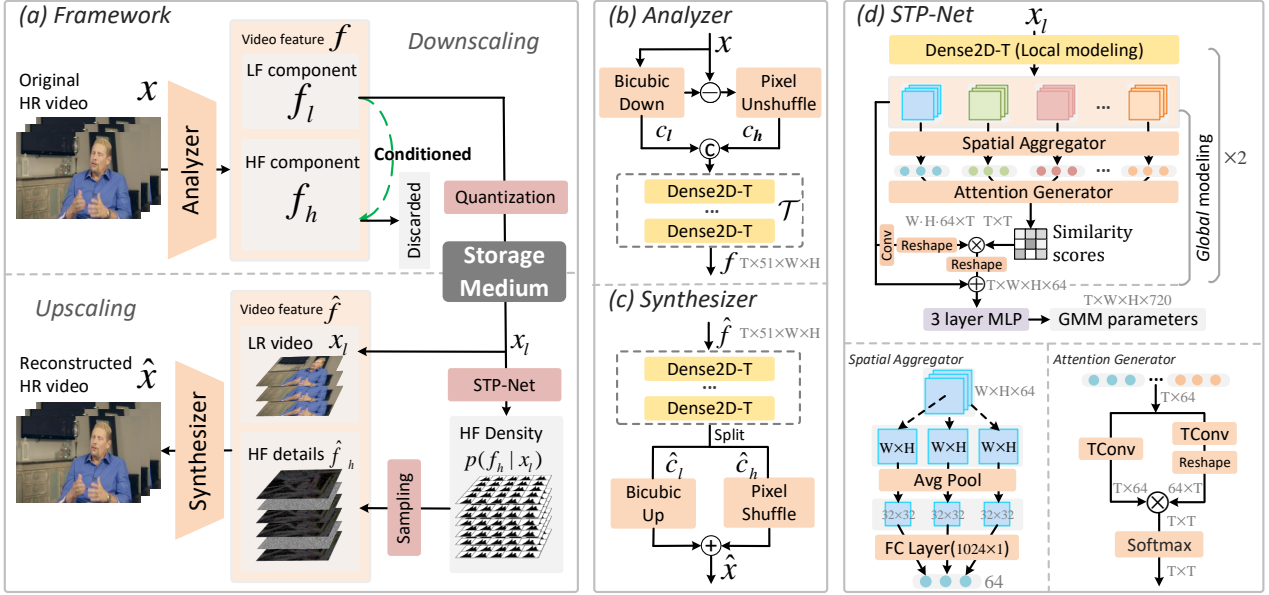


Figure 1: Overview of the proposed framework. We exploit the conditional relationship between different frequency components within the video x for better video rescaling, which are disentangled by the frequency analyzer. During downscaling, the low-frequency (LF) component f_l is quantized to produce the downsampled low-resolution (LR) video x_l . During upscaling, the probability density of the high-frequency (HF) component f_h is predicted by a spatial-temporal prior network (STP-Net). Then, x_l and the sampled HF component \hat{f}_h from the probability distribution is reconstructed to the high-resolution video by the frequency synthesizer. The storage medium can be lossless or lossy for different applications. \odot denotes channel concatenation operation. TConv and Conv represent the 1D convolution with kernel size 1 and the 3D convolution with kernel size $1 \times 1 \times 1$, respectively. The dimensions of some tensors are also indicated, where $W = \frac{w}{k}$, $H = \frac{h}{k}$ and $T = t$.

the HF component \hat{f}_h related to LR video x_l is drawn from the distribution. Finally, we reconstruct the HR video from the concatenation of HF component \hat{f}_h and LR video x_l by the frequency synthesizer (FS).

3.1. Frequency Analyzer and Synthesizer

As shown in Fig. 1 (b), we first decompose the HR input video x as the k times downsampled low-frequency component $c_l := \text{Down}(x) \in \mathbb{R}^{t \times 3 \times \frac{h}{k} \times \frac{w}{k}}$ and the residual high-frequency component $c_h := \text{PixelUnshuffle}(x - \text{Up}(c_l)) \in \mathbb{R}^{t \times 3 \times k^2 \times \frac{h}{k} \times \frac{w}{k}}$, where $h \times w$ denotes the spatial scale of the original video and t denotes the video length. Down and Up represent bicubic downscaling and upscaling operations with scaling ratio k . PixelUnshuffle is the inverse operation of the pixel shuffling operation proposed in [45], where the scaling ratio is also k . Then, we use a learnable transformation \mathcal{T} to transform c_l and c_h to the output features

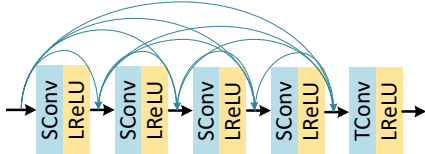


Figure 2: Dense2D-T block. SConv denotes the spatial convolution, i.e., 3D convolution of kernel size $1 \times 3 \times 3$. TConv denotes the temporal convolution, i.e., 3D convolution of kernel size $3 \times 1 \times 1$. LReLU denotes the Leaky ReLU non-linearity [63].

$f := \mathcal{T}(c_l \odot c_h)$, where \odot denotes the channel concatenation operation. Here the produced video feature f consists of LF component f_l and HF component f_h . The network architecture for \mathcal{T} is very flexible in our framework and we use multiple stacking Dense2D-T blocks to implement \mathcal{T} by default. The architecture of Dense2D-T block is shown in Fig. 2, where we extend the vanilla Dense2D block [22] with the temporal modeling ability.

The architecture of frequency synthesizer is symmetric with the analyzer, as shown in Fig. 1 (c). Specifically, we use channel splitting, bicubic upscaling and pixel shuffling operations to synthesize the final high resolution videos based on the reconstructed video feature \hat{f} .

3.2. A Self-conditioned Probabilistic Model

Directly optimizing $p(f_h|x_l)$ in Eq. (1) through gradient descent is unstable due to the unsmooth gradient [26] of the quantization module. Thus, we optimize $p(f_h|f_l)$ instead during training procedure. Specifically, we represent the high-frequency component f_h as a continuous multi-modal probability distribution conditioned on the low-frequency component f_l , which is formulated as:

$$p(f_h|f_l) = \prod_o p(f_h(o)|f_l), \quad (2)$$

where o denotes the spatial-temporal location. We use a continuous Gaussian Mixture Model (GMM) [42] to ap-

proximate p with component number $K = 5$. The distributions are defined by the learnable mixture weights w_o^k , means μ_o^k and log variances σ_o^k . With these parameters, the distributions can be accurately determined as:

$$p(f_h(o)|f_l) = \sum_{k=1}^K w_o^k p_g(f_h(o)|\mu_o^k, e^{\sigma_o^k}), \quad (3)$$

where

$$p_g(f|\mu, \sigma^2) = \frac{1}{\sqrt{\pi}\sigma} e^{-\frac{(f-\mu)^2}{\sigma^2}}, \quad (4)$$

and o denotes the spatial-temporal location.

3.3. Spatial-temporal Prior Network (STP-Net)

As shown in Fig. 1 (d), to estimate the parameters of the distribution above, we propose the STP-Net to model both the local and global temporal information. We first utilize the Dense2D-T block to extract the short term spatial-temporal features for each input frame. In this stage, only information from local frames, *i.e.*, the previous or the next frames, are aggregated into the current frame, while the temporally long-range dependencies in videos are neglected. Therefore, we further introduce the attention mechanism for modeling the global temporal information. More specifically, the spatial dimension of the short-term spatial-temporal features is first reduced by a spatial aggregator, which is implemented as an average pooling operation followed by a full-connected (FC) layer. The output scale of the pooling operation is 32×32 . Then we use dot-producting operation to generate the attention map, which represents the similarity scores between every two frames. Finally, we refine the local spatial-temporal features based on the similarity scores. We repeat the following procedure for 2 times to extract better video features. After that, a 3-layer multi layer perceptron (MLP) is used to estimate the parameters of the GMM distribution, where the linear layers are implemented as 3D convolutions of kernel size $1 \times 1 \times 1$.

3.4. Quantization and Storage Medium

We use rounding operation as the quantization module, and store the output LR videos by lossless format, *i.e.*, H.265 lossless mode. The gradient of the module is calculated by Straight-Through Estimator [4]. We also discuss how to adapt the framework to more practical lossy video formats such as H.264 and H.265 in Section 3.6.

3.5. Training Strategy

Building a learned video rescaling framework is non-trivial, especially the generated low-resolution videos are expected to benefit both the upscaling procedure and the downstream tasks. We consider the following objectives.

Self-conditioned Probability Learning. First, to make sure the STP-Net can obtain an accurate estimation for the HF component f_h , we directly minimize the negative log-likelihood of $p(f_h|f_l)$ in Eq. (2):

$$\mathcal{L}_c = - \sum_{i=0}^N \log(p(f_h^i|f_l^i)), \quad (5)$$

where N is the number of the training samples.

Mimicking Bicubic downscaling. Then the downsampled video is preferred to be similar to the original video, making its deployment for the downstream tasks easier. Therefore, we regularize the the downsampled video before quantization, *i.e.*, f_l , to mimic the bicubic downsampled x :

$$\mathcal{L}_{mimic} = \|x_{bicubic} - f_l\|_2, x_{bicubic} = \text{Bicubic}(x). \quad (6)$$

Penalizing \mathcal{T} . Without any extra constraint, Eq. (5) can be easily minimized by tuning f_h to one constant tensor for any input video. Thus, to avoid the trivial solution, the CNN parts of frequency analyzer and synthesizer are penalized by the photo-parametric loss (*i.e.*, ℓ_2 loss) between the video directly reconstructed from f and the original input x :

$$\mathcal{L}_{pen} = \|x - \text{FS}(f)\|_2. \quad (7)$$

Minimizing reconstruction difference. Finally, the expected difference between the reconstructed video sampled from the model and the original video should be minimized:

$$\mathcal{L}_{recons} = \ell(x, \hat{x}), \hat{x} = \text{FS}(x_l \oplus \hat{f}_h), \quad (8)$$

where ℓ denotes a photo-metric loss (*i.e.*, ℓ_1 loss), \oplus denotes the channel-wise concatenation operation. In each training iteration, \hat{f}_h is sampled from the distribution constructed from the parameters output by STP-Net, conditioning on the LR video x_l . To enable an end-to-end optimization, we apply the “reparametrization trick” [28, 43, 15] to make the sampling procedure differentiable. More details are provided in the supplementary material.

The total loss is then given by:

$$\mathcal{L}_{selfc} = \lambda_1 \mathcal{L}_c + \lambda_2 \cdot k^2 \mathcal{L}_{mimic} + \lambda_3 \mathcal{L}_{pen} + \lambda_4 \mathcal{L}_{recons}, \quad (9)$$

where λ_1 , λ_2 , λ_3 and λ_4 are the balancing parameters, and k is the scaling ratio. The loss function of our framework may seem a little bit complicated. However, we want to mention that the performance of our framework is not sensitive to these hyper-parameters and directly setting all the parameters to 1 already achieves reasonable performance.

3.6. Application I: Video Compression

In this section, we extend the proposed SelfC framework to a lossy video compression system and aim to demonstrate the effectiveness of our approach in reducing the storage size. The whole system is shown in Fig. 3. Specifically, we first use the SelfC framework to generate the downsampled video x_l , which will be compressed by using the existing codecs, *e.g.*, H.265. Then at the decoder side, the compressed videos will be decompressed and upsampled to the full resolution video.

Considering the traditional video codecs are non-differential, we further propose a novel optimization strategy. Specifically, we introduce a differential surrogate video

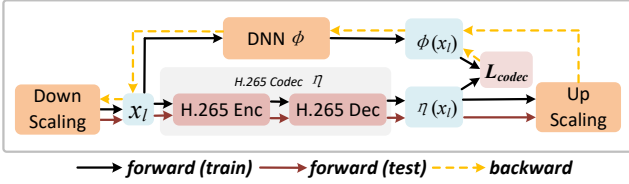


Figure 3: We introduce a surrogate DNN to calculate the gradient of the non-differential codec. We take the H.265 codec as the example.

perturbator ϕ , which is implemented as a deep neural network (DNN) consisting of 6 Dense2D-T blocks. During the back-propagation stage, the gradient of the codec can be approximated by that of ϕ , which is tractable. During the test stage, the surrogate DNN is removed and we directly use the H.265 codec for compression and decompression.

According to the *control variates* theory [12, 14], ϕ can be an low-variance gradient estimator for the video codec (*i.e.*, η) when (1) the differences between the outputs of the two functions are minimized and (2) the correlation coefficients ρ of the two output distributions are maximized.

Therefore, we introduce these two constraints to the optimization procedure of the proposed SelfC based video compression system. And the loss function for the surrogate video perturbator is formulated as:

$$\mathcal{L}_{codec} = \|\eta(x_l) - \phi(x_l)\|_2 - \lambda_\rho \rho(\eta, \phi), \quad (10)$$

where λ_ρ is set to a small value, *i.e.*, 0.001, and ρ is estimated within each batch by Monte Carlo sampling:

$$\rho(\eta, \phi) = \frac{\sum_{k=1}^N (\eta(x_l^k) - \mathbb{E}[\eta])(\phi(x_l^k) - \mathbb{E}[\phi])}{\sqrt{\sum_{k=1}^N (\eta(x_l^k) - \mathbb{E}[\eta])^2} \sqrt{\sum_{k=1}^N (\phi(x_l^k) - \mathbb{E}[\phi])^2}}, \quad (11)$$

where

$$\mathbb{E}[\eta] = \frac{1}{N} \sum_{k=1}^N \eta(x_l^k), \quad \mathbb{E}[\phi] = \frac{1}{N} \sum_{k=1}^N \phi(x_l^k), \quad (12)$$

and N denotes the batch size. Finally, the total loss function for the SelfC based video compression system is given by:

$$\mathcal{L}_{compression} = \mathcal{L}_{selfc} + \mathcal{L}_{codec}. \quad (13)$$

3.7. Application II: Efficient Action Recognition

We further apply the proposed SelfC framework to the video action recognition task. Specifically, we adopt the LR videos (*i.e.*, x_l) downscaled by our framework as the input of action recognition CNNs for efficient action recognition. Considering the downscaler of our approach can preserve meaningful information for the downstream tasks and the complexity of itself can be rather low, inserting the downscaler before the off-the-shelf action CNNs can reduce the huge computational complexity of them with negligible performance drop. Moreover, the light-weightness of the rescaling framework makes the joint optimization tractable. In fact, compared with bicubic downscaling operation, our downscaler in SelfC framework can still generate more informative low-resolution videos for the action recognition task even without the joint training procedure. Please see Section 4.5 for more experimental results.

4. Experiments

4.1. Dataset

We use Vimeo90K dataset [65] as our training data, which is also adopted by the recent video super resolution methods [23, 24, 59] and video compression methods [34, 20, 33]. For *video rescaling task*, the evaluation datasets are the test set of Vimeo90K (denoted by Vimeo90K-T), the widely-used Vid4 benchmark [32] and SPMCs-30 dataset [50]. For *video compression task*, the evaluation datasets include UVG [1], MCL-JCV [57], VTL [2] and HEVC Class B [48]. For *video recognition task*, we train and evaluate it on two large scale datasets requiring temporal relation reasoning, *i.e.*, Something V1&V2 [13][38].

4.2. Implementation Details

(1) Video rescaling: λ_1 , λ_2 , λ_3 and λ_4 are set as 0.1, 1, 1 and 1, respectively. Each training clip consists of 7 RGB patches of size 256×256 . The batch size is set as 32. We augment the training data with random horizontal flips and 90° rotations. We train our model with Adam optimizer [27] by setting β_1 as 0.9, β_2 as 0.99, and learning rate as 10^{-4} . The total training iteration number is about 240,000. The learning rate is divided by 10 every 100,000 iterations. We implement the models with the PyTorch framework [39] and train them on a server with 8 NVIDIA 2080Ti GPUs. We draw 5 times from the generated distribution for each evaluation and report the averaged performance. We leverage the invertible neural network (INN) architecture to implement the CNN parts of the paired frequency analyzer and synthesizer for fair comparison with IRN on parameter number because INN will cut the number of parameters by 50%. We propose the two following models: the SelfC-*small* and SelfC-*large*, which consist of 2 and 8 invertible Dense2D-T blocks respectively. The detailed architecture of this block is in the supplementary material, roughly following [62]. Training the SelfC-*large* model takes about 90 hours.

(2) Video compression: The rescaling ratio of the SelfC is set to 2. We use H.265 as our default codec in the experiments. λ_2 is set as 100 to make sure the statistical distribution of the downscaled videos is more closed to the natural images, which stabilizes the performance of the whole system. The other details follow that of video rescaling task. The models are initialized from SelfC-*large* model but the number of invertible Dense2D-T blocks is reduced to 4. The surrogate CNN is randomly initialized, and are jointly optimized with video rescaler.

(3) Action recognition: We insert the downscaler of our framework before the action recognition CNN (*i.e.*, TSM [30]). The data augmentation pipeline also follows TSM. The downscaling ratio is 2. At inference time, we used just 1 clip per video and each clip contains 8 frames. We adopt 2 plain Dense2D-T blocks with interme-

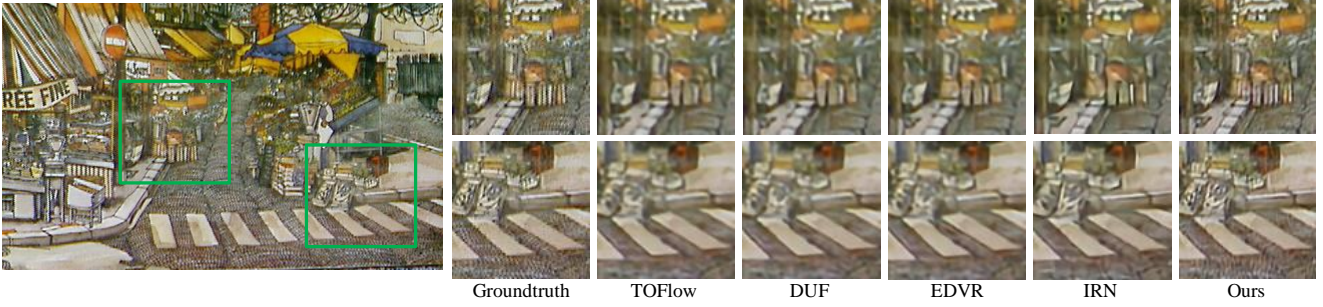


Figure 4: Qualitative comparison on the reconstruction of 4 \times downsampled *calendar* clip. *Best to view by zooming in.*

Downscaling	Upscaling	#Frame	FLOPs	#Param.	Calendar (Y)	City (Y)	Foliage (Y)	Walk (Y)	Vid4-avg(Y)	Vid4-avg(RGB)
Bicubic	Bicubic	1	N/A	N/A	18.83/0.4936	23.84/0.5234	21.52/0.4438	23.01/0.7096	21.80/0.5426	20.37/0.5106
Bicubic	SPMC [50]	3	-	-	-/-	-/-	-/-	-/-	25.52/0.76	-/-
Bicubic	Liu [32]	5	-	-	21.61/-	26.29/-	24.99/-	28.06/-	25.23/-	-/-
Bicubic	TOFlow [65]	7	0.81T	1.41M	22.29/0.7273	26.79/0.7446	25.31/0.7118	29.02/0.8799	25.85/0.7659	24.39/0.7438
Bicubic	FRVSR [44]	2	0.14T	5.05M	22.67/0.7844	27.70/0.8063	25.83/0.7541	29.72/0.8971	26.48/0.8104	25.01/0.7917
Bicubic	DUF-52L [25]	7	0.62T	5.82M	24.17/0.8161	28.05/0.8235	26.42/0.7758	30.91/0.9165	27.38/0.8329	25.91/0.8166
Bicubic	RBP [18]	7	9.30T	12.2M	24.02/0.8088	27.83/0.8045	26.21/0.7579	30.62/0.9111	27.17/0.8205	25.65/0.7997
Bicubic	EDVR-L [59]	7	0.93T	20.6M	24.05/0.8147	28.00/0.8122	26.34/0.7635	31.02/0.9152	27.35/0.8264	25.83/0.8077
Bicubic	PFNL [69]	7	0.70T	3.00M	23.56/0.8232	28.11/0.8366	26.42/0.7761	30.55/0.9103	27.16/0.8365	25.67/0.8189
Bicubic	RLSP [11]	3	0.09T	4.21M	24.36/0.8235	28.22/0.8362	26.66/0.7821	30.71/0.9134	27.48/0.8388	25.69/0.8153
Bicubic	TGA [24]	7	0.23T	5.87M	24.50/0.8285	28.50/0.8442	26.59/0.7795	30.96/0.9171	27.63/0.8423	26.14/0.8258
Bicubic	RSDN 9-128 [23]	2	0.13T	6.19M	24.60/0.8355	29.20/0.8527	26.84/0.7931	31.04/0.9210	27.92/0.8505	26.43/0.8349
IRN	IRN [62]	1	0.20T	4.36M	25.05/0.8424	29.84/0.8825	28.79/0.8604	34.24/0.9584	29.48/0.8859	27.58/0.8618
SelfC-small	SelfC-small	7	0.026T	0.68M	26.02/0.8675	30.26/0.8953	29.73/0.8829	34.87/0.9747	30.28/0.9021	27.98/0.8763
SelfC-large	SelfC-large	7	0.093T	2.65M	27.12/0.9018	31.16/0.9171	30.59/0.9123	35.56/0.9730	31.11/0.9261	29.06/0.9065

Table 1: Quantitative comparison (PSNR (dB) and SSIM) on Vid4 for 4 \times video rescaling. Y indicates the luminance channel. FLOPs (MAC) are calculated on an HR frame of size 720 \times 480.

Downscaling	Bicubic	Bicubic	Bicubic	Bicubic	Bicubic	Bicubic	Bicubic	IRN	SelfC-small	SelfC-large
Upscaling	Bicubic	TOFlow [65]	FRVSR [44]	DUF-52L [25]	RBPn [18]	PFNL[69]	RSDN 9-128 [23]	IRN [62]	SelfC-small	SelfC-large
SPMCs-30(Y)	23.29/0.6385	27.86/0.8237	28.16/0.8421	29.63/0.8719	29.73/0.8663	29.74/0.8792	-/-	34.45/0.9358	34.51/0.9372	37.86/0.9710
SPMCs-30(RGB)	21.83/0.6133	26.38/0.8072	26.68/0.8271	28.10/0.8582	28.23/0.8561	27.24/0.8495	-/-	32.26/0.9185	32.33/0.9201	35.19/0.9567
Vimeo90K-T(Y)	31.30/0.8687	34.62/0.9212	35.64/0.9319	36.87/0.9447	37.20/0.9458	-/-	37.23/0.9471	37.47/0.9686	37.18/0.9701	38.08/0.9762
Vimeo90K-T(RGB)	29.77/0.8490	32.78/0.9040	33.96/0.9192	34.96/0.9313	35.39/0.9340	-/-	35.32/0.9344	35.14/0.9535	35.02/0.9542	35.55/0.9627

Table 2: Quantitative comparison (PSNR(dB) and SSIM) on SPMCs-30 and Vimeo90K-T for 4 \times video rescaling.

diate channel number of 12 as the CNN part of frequency analyzer. Note that the downscaler is first pretrained on Vimeo90K dataset by the video rescaling task.

4.3. Results of Video Rescaling

As shown in Tab. 1 and Tab. 2, our method outperforms the recent state-of-the-art video super resolution methods on Vid4, SPMCs-30 and Vimeo90K-T by a large margin in terms of both PSNR and SSIM. For example, the average PSNR(Y) results on the Vid4 dataset for our SelfC-large is 31.11dB, while the corresponding result for the state-of-the-art video super resolution approach RSDN is only 27.92dB. Furthermore, we also provide the results of image rescaling method, *i.e.*, IRN, in Tab. 1 and Tab. 2. It is obvious that our method outperforms IRN while also reduces the computational complexity by 2 times (SelfC-large) or 8 times (SelfC-small). This result clearly demonstrates that it is necessary to exploit the temporal relationship for video rescaling task, while the existing image rescaling methods like IRN ignored this temporal cue. We also show the qual-

itative comparison with other methods on Vid4 in Fig. 4. Please refer to the supplementary material for more qualitative results. Our method demonstrates much better details and sharper images than both video super-resolution methods and image rescaling method, proving the superiority of the video rescaling paradigm.

4.4. Results of Video Compression

For fair comparison, both the standard H.265 codec and the codec embedded in our framework follow the same setting in [34] and use the FFmpeg with very fast mode. The evaluation metrics are PSNR and MS-SSIM [60].

Fig. 5 shows the experimental results on the UVG and MCL-JCV datasets. It is obvious that our method outperforms both the traditional methods and learning based method on video compression task by a large margin. On the UVG dataset, the proposed method achieves about 0.8dB gain at the same Bpp level in comparison with H.265. Although our method is only optimized by ℓ_1 loss, it demonstrates strong performances in terms of both PSNR

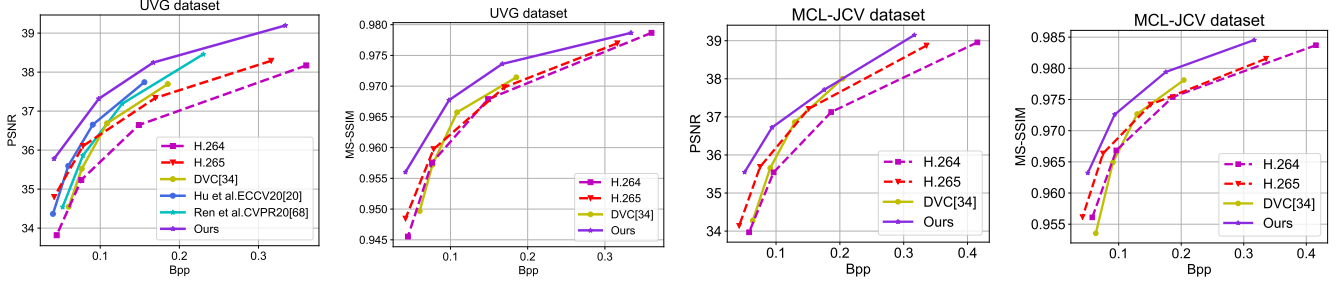


Figure 5: Comparison between the proposed method with H.265, H.264 and the learning based video codec DVC [34].

Dataset	UVG	VTL	MCL-JCV	Average
BDBR by PSNR	-39.86	-27.45	-16.75	-28.02
BDBR by MS-SSIM	-29.01	-14.42	-26.59	-23.34

Table 3: BDBR results using H.265 as the anchor. The lower value, the more bit cost reduced.

and MS-SSIM metrics.

We also evaluate the Bjøntegaard Delta Bit-Rate (BDBR) [5] by using H.265 as the anchor method, and calculate the average bit-rate difference at the same PSNR or MS-SSIM, which indicates the storage burden reduction quantitatively. As shown in Tab. 3, our method saves the bit cost by over 25% averagely under the same PSNR and over 20% under the same MS-SSIM. Notably, we reduce the bit cost by about 40% on UVG dataset. This proves that video rescaling technique is a novel and effective way to improve the video compression performance, without considering much about the complicated details of the codecs, especially for the industrial lossy codecs.

We perform more analysis to verify the effectiveness of the “Video rescaling+Codec” paradigm and the proposed gradient estimation method. As shown in Fig. 6, it is observed that using Bicubic as the downscaler and upscaler in the video compression system (*i.e.*, H.265+Bicubic) leads to much inferior result than the baseline. We also try to improve the result by using a state-of-the-art video super resolution method, *i.e.*, TGA [24]. The performance is indeed improved though still lower than the baseline method H.265. Considering the network parameters of TGA are 5.87M while ours are only 2.65M, this result further demonstrates the effectiveness of our SelfC framework. Finally, we provide experimental results (*i.e.*, Ours W/O Gradient) when directly using the biased Straight-Through Estimator [4] for H.265 codec. The results show that the proposed gradient estimation method in Section 3.6 can bring nearly 0.3dB improvements.

4.5. Results of Efficient Video Action Recognition

We show the video action recognition results in Tab. 4. In the first group, when directly testing the action model pretrained on full resolution videos, we observe the performances of low-resolution videos downsampled by Bicubic and ours are both dropped drastically, because the classi-

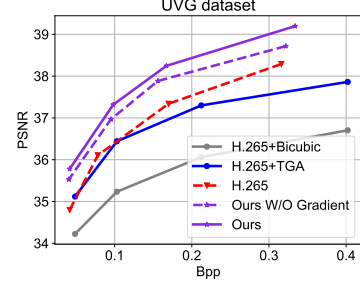


Figure 6: Comparison of our “Video rescaling+Codec” scheme with other paradigms.

fication networks are rather sensitive to the absolute scale of the input. However, our downscaler still performs better (30.4% vs. 32.7% on Something V1 dataset).

In the second group, we provide the experimental results when the action recognition CNN is fine-tuned on the low-resolution videos from Bicubic and our downscaler in SelfC. The details of fine-tuning procedure are in the supplementary material. It is obvious that our method clearly outperforms bicubic downscaling by about 1.5% in terms of Top1 accuracy on the two datasets. Notably, our downscaler is learnable. Therefore, we then fine-tune action recognition CNNs and our downscaler jointly. The results are in the third group. The end-to-end joint training further improves the performance by an obvious margin. On Something V2, the ultimate performances of our method nearly achieve that of performing recognition directly on HR videos, and our method improves the efficiency by over 3 times. The downscaler of IRN can not improve the efficiency of this task because its computation cost is even larger than the **HR** setting. We try to decrease the layer

Method	Action CNN	FLOPs	Params	v1		v2	
				Top1 (%)	Top5 (%)	Top1 (%)	Top5 (%)
HR	TSM	33G	24.31M	45.6	74.2	58.8	85.4
Bicubic	TSM	8.6G	24.31M	30.4	57.5	40.1	68.7
Ours	TSM	10.8G	24.35M	32.7	59.5	41.8	71.5
Bicubic (FT)	TSM	8.6G	24.31M	42.1	72.1	56.0	83.9
Ours (FT)	TSM	10.8G	24.35M	43.5	72.8	57.4	84.8
Ours (E2E)	TSM	10.8G	24.35M	44.6	73.3	58.3	85.5

Table 4: Comparison between our method and Bicubic downscaler. FT denotes only fine-tuning the action recognition CNN. E2E denotes also fine-tuning the downscaler.

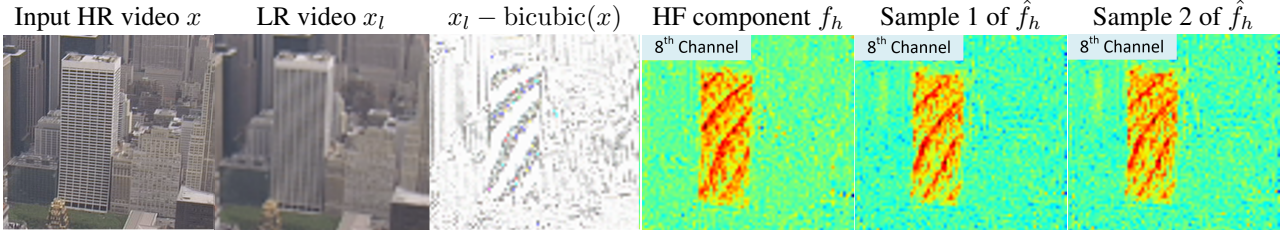


Figure 7: Visualization of the high-frequency component \hat{f}_h sampled from the learned distribution $p(f_h|x_l)$. We also compare the difference of the downsampled video by ours and Bicubic. Since the magnitude of the difference is small, we amplify it by 10 times for better visualization.

number of IRN but it no longer converges.

4.6. Ablation Studies on the Framework

In this section, we conduct experiments on video rescaling task to verify the effectiveness of the components in our framework. We first define the following 2 baselines: (1) IRN [62], which is the most recent state-of-the-art image rescaling method. For fair comparison, we retrain it on Vimeo90K dataset using the codes open-sourced by the authors. (2) Auto-Enc, which is a simple auto encoder-decode architecture by removing the STP-Net of our model. The experimental results are shown in Tab. 5.

Methods	Backbone	Probability model	Param(M)	Vid4(Y)	
				PSNR(dB)	SSIM
Auto-Enc	16×Dense2D-T	-	3.63	27.82	0.8297
IRN	16×Dense2D	Normal	4.36	29.48	0.8859
IRN*	16×Dense2D-T	Normal	3.63	29.01	0.8786
SelfC-basic	2×Dense2D	GMM(K=1)	0.73	29.22	0.8842
SelfC-basicT	2×Dense2D-T	GMM(K=1)	0.64	29.67	0.8864
SelfC-small	2×Dense2D-T	GMM(K=5)	0.68	30.28	0.9021
SelfC-large	8×Dense2D-T	GMM(K=5)	2.65	31.11	0.9261

Table 5: Ablation studies on 4× video rescaling. All blocks adopt the INN architecture for fair comparison with IRN.

First, the Auto-Enc baseline shows more inferior performance than both IRN and our method. This proves that explicitly modeling the lost information is important. IRN is inferior to our *small* model although IRN leverages an 8 times heavier backbone. We also tried to equip IRN with the temporal modeling ability by replacing its backbone from Dense2D to Dense2D-T. Surprisingly, the performance of the new model IRN* decreases by 0.47dB. The reason is that IRN relies on the complex non-linear transformation to transform the real distribution of the lost information to the normal distribution while the transformation ability of the Dense2D-T is weaker (missing 0.73M parameters).

For our method, we start from the most simple model denoted by SelfC-basic, where backbone consists of only spatial convolutions, and the STP-Net only outputs a simple Gaussian distribution. The performance of this model is comparable with IRN but with 6× fewer parameters. This proves the efficiency and superiority of the proposed self-conditioned distribution modeling scheme. Then, we introduce an improved model denoted by SelfC-basicT. The

temporal modeling ability of it is stronger by changing the basic block from Dense2D to Dense2D-T. This leads to 0.45dB improvement while reducing the parameters, proving the effectiveness of the Dense2D-T block for video task. Further, we increase the mixture number of the GMM model to 5. The resulted SelfC-*small* model outperforms all the baselines by a large margin (30.28dB) with only 0.68M parameters. Our model is also scalable with larger backbone network. Enlarging that by 4 times improves the performance by 0.83dB. For more ablation studies on the depth of backbone network, comparison of different probabilistic modeling methods, the architecture of the STP-Net and the loss functions, please refer to the supplementary material.

4.7. Visualization Results

While the previous quantitative results validate the superiority of the proposed self-conditioned modeling scheme on several tasks, it is interesting to investigate the intermediate components output by our model, especially the distribution of the high-frequency (HF) component predicted by STP-Net. Note that the distribution is a mixture of Gaussian and includes multiple channels, we draw two samples of \hat{f}_h from $p(f_h|x_l)$ and randomly select 1 channel of them for visualization. The f_h output from the frequency analyzer is adopted as the ground-truth sample.

As shown in Fig. 7, we first see that the LR video x_l downsampled by our method is modulated into some mandatory information for reconstructing the HF components more easily, compared to Bicubic. Also, the sampled HF components can restore the ground-truth of that accurately in terms of key structures, *i.e.*, the windows of the building, while retaining a certain degree of the randomness. This is consistent with our learning objectives.

5. Conclusion

We have proposed a video-rescaling framework to learn a pair of downscaling and upscaling operations. Extensive experiments demonstrated that our method can outperform the previous methods with a large margin while with much fewer parameters and computational cost. Moreover, the learned downscaling operator facilitates the tasks of video compression and efficient action recognition significantly.

References

- [1] Ultra video group test sequences. <http://ultravideo.cs.tut.fi>, accessed: 2019- 11-06. **5**
- [2] Video trace library. <http://trace.kom.aau.dk/yuv/index.html>, accessed: 2019- 11-06. **5**
- [3] Eirikur Agustsson, David Minnen, Nick Johnston, Johannes Balle, Sung Jin Hwang, and George Toderici. Scale-space flow for end-to-end optimized video compression. In *Proceedings of the IEEE/CVF Conference on Computer Vision and Pattern Recognition*, pages 8503–8512, 2020. **2**
- [4] Yoshua Bengio, Nicholas Léonard, and Aaron Courville. Estimating or propagating gradients through stochastic neurons for conditional computation. *arXiv*, 2013. **4, 7**
- [5] Gisle Bjontegaard. Calculation of average psnr differences between rd-curves. *VCEG-M33*, 2001. **7**
- [6] Joao Carreira and Andrew Zisserman. Quo vadis, action recognition? a new model and the kinetics dataset. In *CVPR*, 2017. **2**
- [7] Abdelaziz Djelouah, Joaquim Campos, Simone Schaub-Meyer, and Christopher Schroers. Neural inter-frame compression for video coding. In *Proceedings of the IEEE/CVF International Conference on Computer Vision*, pages 6421–6429, 2019. **2**
- [8] Yin Fan, Xiangju Lu, Dian Li, and Yuanliu Liu. Video-based emotion recognition using cnn-rnn and c3d hybrid networks. In *Proceedings of the 18th ACM international conference on multimodal interaction*, pages 445–450, 2016. **1**
- [9] Christoph Feichtenhofer, Haoqi Fan, Jitendra Malik, and Kaiming He. Slowfast networks for video recognition. In *ICCV*, 2019. **2**
- [10] Christoph Feichtenhofer, Axel Pinz, and Andrew Zisserman. Convolutional two-stream network fusion for video action recognition. In *CVPR*, 2016. **2**
- [11] Dario Fuoli, Shuhang Gu, and Radu Timofte. Efficient video super-resolution through recurrent latent space propagation. In *ICCVW*, 2019. **6**
- [12] Peter W Glynn and Roberto Szechtman. Some new perspectives on the method of control variates. In *Monte Carlo and Quasi-Monte Carlo Methods 2000*. 2002. **5**
- [13] Raghav Goyal, Samira Ebrahimi Kahou, Vincent Michalski, Joanna Materzynska, Susanne Westphal, Heuna Kim, Valentin Haenel, Ingo Fruend, Peter Yianilos, Moritz Mueller-Freitag, et al. The” something something” video database for learning and evaluating visual common sense. In *ICCV*, 2017. **5**
- [14] Will Grathwohl, Dami Choi, Yuhuai Wu, Geoffrey Roeder, and David Duvenaud. Backpropagation through the void: Optimizing control variates for black-box gradient estimation. *arXiv*, 2017. **5**
- [15] Alex Graves. Stochastic backpropagation through mixture density distributions. *arXiv*, 2016. **4**
- [16] Amirhossein Habibi, Ties van Rozendaal, Jakub M Tomczak, and Taco S Cohen. Video compression with rate-distortion autoencoders. In *Proceedings of the IEEE/CVF International Conference on Computer Vision*, pages 7033–7042, 2019. **2**
- [17] Kensho Hara, Hirokatsu Kataoka, and Yutaka Satoh. Learning spatio-temporal features with 3d residual networks for action recognition. In *ICCVW*, 2017. **2**
- [18] Muhammad Haris, Gregory Shakhnarovich, and Norimichi Ukita. Recurrent back-projection network for video super-resolution. In *CVPR*, 2019. **2, 6**
- [19] Kaiming He, Xiangyu Zhang, Shaoqing Ren, and Jian Sun. Deep residual learning for image recognition. In *CVPR*, 2016. **2**
- [20] Zhihao Hu, Zhenghao Chen, Dong Xu, Guo Lu, Wanli Ouyang, and Shuhang Gu. Improving deep video compression by resolution-adaptive flow coding. In *ECCV*, 2020. **5**
- [21] Zhihao Hu, Guo Lu, and Dong Xu. Fvc: A new framework towards deep video compression in feature space. In *Proceedings of the IEEE/CVF Conference on Computer Vision and Pattern Recognition*, pages 1502–1511, 2021. **2**
- [22] Forrest Iandola, Matt Moskewicz, Sergey Karayev, Ross Girshick, Trevor Darrell, and Kurt Keutzer. Densenet: Implementing efficient convnet descriptor pyramids. In *arXiv*, 2014. **3**
- [23] Takashi Isobe, Xu Jia, Shuhang Gu, Songjiang Li, Shengjin Wang, and Qi Tian. Video super-resolution with recurrent structure-detail network. In *ECCV*, 2020. **5, 6**
- [24] Takashi Isobe, Songjiang Li, Xu Jia, Shanxin Yuan, Gregory Slabaugh, Chunjing Xu, Ya-Li Li, Shengjin Wang, and Qi Tian. Video super-resolution with temporal group attention. In *CVPR*, 2020. **5, 6, 7**
- [25] Younghyun Jo, Seoung Wug Oh, Jaeyeon Kang, and Seon Joo Kim. Deep video super-resolution network using dynamic upsampling filters without explicit motion compensation. In *CVPR*, 2018. **2, 6**
- [26] Heewon Kim, Myungsub Choi, Bee Lim, and Kyoung Mu Lee. Task-aware image downscaling. In *ECCV*, 2018. **1, 2, 3**
- [27] Diederik P Kingma and Jimmy Ba. Adam: A method for stochastic optimization. In *arXiv*, 2014. **5**
- [28] Diederik P Kingma and Max Welling. Auto-encoding variational bayes. *arXiv*, 2013. **4**
- [29] Yue Li, Dong Liu, Houqiang Li, Li Li, Zhu Li, and Feng Wu. Learning a convolutional neural network for image compact-resolution. In *TIP*, 2018. **1, 2**
- [30] Ji Lin, Chuhan Gan, and Song Han. Tsm: Temporal shift module for efficient video understanding. In *ICCV*, 2019. **2, 5**
- [31] Jianping Lin, Dong Liu, Houqiang Li, and Feng Wu. M-lvc: multiple frames prediction for learned video compression. In *Proceedings of the IEEE/CVF Conference on Computer Vision and Pattern Recognition*, pages 3546–3554, 2020. **2**
- [32] Ce Liu and Deqing Sun. On bayesian adaptive video super resolution. In *TPAMI*, 2013. **1, 2, 5, 6**
- [33] Guo Lu, Chunlei Cai, Xiaoyun Zhang, Li Chen, Wanli Ouyang, Dong Xu, and Zhiyong Gao. Content adaptive and error propagation aware deep video compression. In *ECCV*, 2020. **2, 5**
- [34] Guo Lu, Wanli Ouyang, Dong Xu, Xiaoyun Zhang, Chunlei Cai, and Zhiyong Gao. Dvc: An end-to-end deep video compression framework. In *CVPR*, 2019. **2, 5, 6, 7**

- [35] Guo Lu, Wanli Ouyang, Dong Xu, Xiaoyun Zhang, Zhiyong Gao, and Ming-Ting Sun. Deep kalman filtering network for video compression artifact reduction. In *Proceedings of the European Conference on Computer Vision (ECCV)*, pages 568–584, 2018. 1
- [36] Guo Lu, Xiaoyun Zhang, Wanli Ouyang, Li Chen, Zhiyong Gao, and Dong Xu. An end-to-end learning framework for video compression. *IEEE transactions on pattern analysis and machine intelligence*, 2020. 2
- [37] Guo Lu, Xiaoyun Zhang, Wanli Ouyang, Dong Xu, Li Chen, and Zhiyong Gao. Deep non-local kalman network for video compression artifact reduction. *IEEE Transactions on Image Processing*, 29:1725–1737, 2019. 1
- [38] Farzaneh Mahdisoltani, Guillaume Berger, Waseem Gharbieh, David Fleet, and Roland Memisevic. Fine-grained video classification and captioning. In *arXiv*, 2018. 5
- [39] Adam Paszke, Sam Gross, Francisco Massa, Adam Lerer, James Bradbury, Gregory Chanan, Trevor Killeen, Zeming Lin, Natalia Gimelshein, Luca Antiga, et al. Pytorch: An imperative style, high-performance deep learning library. In *NeurIPS*, 2019. 5
- [40] Javier Portilla, Vasily Strela, Martin J Wainwright, and Eero P Simoncelli. Image denoising using scale mixtures of gaussians in the wavelet domain. In *TIP*, 2003. 2
- [41] Zhaofan Qiu, Ting Yao, and Tao Mei. Learning spatiotemporal representation with pseudo-3d residual networks. In *ICCV*, 2017. 2
- [42] Douglas A Reynolds. Gaussian mixture models. In *EOB*, 2009. 3
- [43] Danilo Jimenez Rezende, Shakir Mohamed, and Daan Wierstra. Stochastic backpropagation and approximate inference in deep generative models. In *ICML*, 2014. 4
- [44] Mehdi SM Sajjadi, Raviteja Vemulapalli, and Matthew Brown. Frame-recurrent video super-resolution. In *CVPR*, 2018. 6
- [45] Wenzhe Shi, Jose Caballero, Ferenc Huszár, Johannes Totz, Andrew P Aitken, Rob Bishop, Daniel Rueckert, and Zehan Wang. Real-time single image and video super-resolution using an efficient sub-pixel convolutional neural network. In *CVPR*, 2016. 3
- [46] Karen Simonyan and Andrew Zisserman. Two-stream convolutional networks for action recognition in videos. In *NeurIPS*, 2014. 1, 2
- [47] Vasily Strela, Javier Portilla, and Eero P Simoncelli. Image denoising using a local gaussian scale mixture model in the wavelet domain. In *Wavelet Applications in Signal and Image Processing VIII*, 2000. 2
- [48] Gary J Sullivan, Jens-Rainer Ohm, Woo-Jin Han, and Thomas Wiegand. Overview of the high efficiency video coding (hevc) standard. *TCSVT*, 2012. 2, 5
- [49] Wanjie Sun and Zhenzhong Chen. Learned image downscaling for upscaling using content adaptive resampler. In *TIP*, 2020. 1
- [50] Xin Tao, Hongyun Gao, Renjie Liao, Jue Wang, and Jiaya Jia. Detail-revealing deep video super-resolution. In *ICCV*, 2017. 1, 2, 5, 6
- [51] Yuan Tian, Zhaohui Che, Wenbo Bao, Guangtao Zhai, and Zhiyong Gao. Self-supervised motion representation via scattering local motion cues. In *Computer Vision—ECCV 2020: 16th European Conference, Glasgow, UK, August 23–28, 2020, Proceedings, Part XIV 16*, pages 71–89. Springer, 2020. 2
- [52] Yuan Tian, Xiongkuo Min, Guangtao Zhai, and Zhiyong Gao. Video-based early asd detection via temporal pyramid networks. In *2019 IEEE International Conference on Multi-media and Expo (ICME)*, pages 272–277. IEEE, 2019. 1
- [53] Du Tran, Lubomir Bourdev, Rob Fergus, Lorenzo Torresani, and Manohar Paluri. Learning spatiotemporal features with 3d convolutional networks. In *ICCV*, 2015. 2
- [54] Du Tran, Heng Wang, Lorenzo Torresani, Jamie Ray, Yann LeCun, and Manohar Paluri. A closer look at spatiotemporal convolutions for action recognition. In *CVPR*, 2018. 2
- [55] Martin J Wainwright and Eero Simoncelli. Scale mixtures of gaussians and the statistics of natural images. In *NeurIPS*, 1999. 2
- [56] Martin J Wainwright, Eero P Simoncelli, and Alan S Willsky. Random cascades on wavelet trees and their use in analyzing and modeling natural images. In *ACHA*, 2001. 2
- [57] Haiqiang Wang, Weihao Gan, Sudeng Hu, Joe Yuchieh Lin, Lina Jin, Longguang Song, Ping Wang, Ioannis Katsavounidis, Anne Aaron, and C-C Jay Kuo. Mcl-jvc: a jnd-based h. 264/avc video quality assessment dataset. In *ICIP*, 2016. 5
- [58] Limin Wang, Yuanjun Xiong, Zhe Wang, Yu Qiao, Dahua Lin, Xiaoou Tang, and Luc Van Gool. Temporal segment networks for action recognition in videos. In *TPAMI*, 2018. 2
- [59] Xintao Wang, Kelvin CK Chan, Ke Yu, Chao Dong, and Chen Change Loy. Edvr: Video restoration with enhanced deformable convolutional networks. In *CVPRW*, 2019. 1, 2, 5, 6
- [60] Zhou Wang, Eero P Simoncelli, and Alan C Bovik. Multi-scale structural similarity for image quality assessment. In *ACSSC*, 2003. 6
- [61] Thomas Wiegand, Gary J Sullivan, Gisle Bjontegaard, and Ajay Luthra. Overview of the h. 264/avc video coding standard. *TCSVT*, 2003. 2
- [62] Mingqing Xiao, Shuxin Zheng, Chang Liu, Yaolong Wang, Di He, Guolin Ke, Jiang Bian, Zhouchen Lin, and Tie-Yan Liu. Invertible image rescaling. In *ECCV*, 2020. 1, 2, 5, 6, 8
- [63] Bing Xu, Naiyan Wang, Tianqi Chen, and Mu Li. Empirical evaluation of rectified activations in convolutional network. In *arXiv*, 2015. 3
- [64] Zhongwen Xu, Yi Yang, and Alex G Hauptmann. A discriminative cnn video representation for event detection. In *Proceedings of the IEEE conference on computer vision and pattern recognition*, pages 1798–1807, 2015. 1
- [65] Tianfan Xue, Baian Chen, Jiajun Wu, Donglai Wei, and William T Freeman. Video enhancement with task-oriented flow. In *IJCV*, 2019. 1, 2, 5, 6
- [66] Zhicong Yan, Gaolei Li, Yuan Tian, Jun Wu, Shenghong Li, Mingzhe Chen, and H Vincent Poor. Dehib: Deep hidden backdoor attack on semi-supervised learning via adversarial

perturbation. In *Proceedings of the AAAI Conference on Artificial Intelligence*, volume 35, pages 10585–10593, 2021.

1

- [67] Fengting Yang, Qian Sun, Hailin Jin, and Zihan Zhou. Superpixel segmentation with fully convolutional networks. In *Proceedings of the IEEE/CVF Conference on Computer Vision and Pattern Recognition*, pages 13964–13973, 2020. 2
- [68] Ren Yang, Fabian Mentzer, Luc Van Gool, and Radu Timofte. Learning for video compression with hierarchical quality and recurrent enhancement. In *Proceedings of the IEEE/CVF Conference on Computer Vision and Pattern Recognition*, pages 6628–6637, 2020. 2
- [69] Peng Yi, Zhongyuan Wang, Kui Jiang, Junjun Jiang, and Jiayi Ma. Progressive fusion video super-resolution network via exploiting non-local spatio-temporal correlations. In *ICCV*, 2019. 6